Molecular Biology of the Cell
Vol. 18, 2646–2655, July 2007

PI4P Promotes the Recruitment of the GGA Adaptor Proteins to the *Trans*-Golgi Network and Regulates Their Recognition of the Ubiquitin Sorting Signal

Jing Wang,*† Hui-Qiao Sun,*† Eric Macia,‡ Tomas Kirchhausen,‡ Hadiya Watson,§ Juan S. Bonifacino,§ and Helen L. Yin*

*Department of Physiology, University of Texas Southwestern Medical Center at Dallas, Dallas, TX 75390; ‡Department of Cell Biology and Center for Blood Research Institute for Biomedical Research, Harvard Medical School, Boston, MA 02115; and §Cell Biology and Metabolism Branch, National Institute of Child Health and Human Development, National Institutes of Health, Bethesda, MD 20892

Submitted October 5, 2006; Revised April 3, 2007; Accepted April 26, 2007
Monitoring Editor: Sandra Schmid

Phosphatidylinositol 4 phosphate (PI4P) is highly enriched in the *trans*-Golgi network (TGN). Here we establish that PI4P is a key regulator of the recruitment of the GGA clathrin adaptor proteins to the TGN and that PI4P has a novel role in promoting their recognition of the ubiquitin (Ub) sorting signal. Knockdown of PI4KIIα by RNA interference (RNAi), which depletes the TGN's PI4P, impaired the recruitment of the GGAs to the TGN. GGAs bind PI4P primarily through their GAT domain, in a region called C-GAT, which also binds Ub but not Arf1. We identified two basic residues in the GAT domain that are essential for PI4P binding in vitro and for the recruitment of GGAs to the TGN in vivo. Unlike wild-type GGA, GGA with mutated GATs failed to rescue the abnormal TGN phenotype of the GGA RNAi-depleted cells. These residues partially overlap with those that bind Ub, and PI4P increased the affinity of the GAT domain for Ub. Because the recruitment of clathrin adaptors and their cargoes to the TGN is mediated through a web of low-affinity interactions, our results show that the dual roles of PI4P can promote specific GGA targeting and cargo recognition at the TGN.

INTRODUCTION

Phosphatidylinositol 4 phosphate (PI4P) has recently emerged as a *trans*-Golgi network (TGN) marker that establishes a signpost for the recruitment of trafficking proteins (Behnia and Munro, 2005; Carlton and Cullen, 2005). Recently, we found that the major TGN clathrin adaptor, AP-1, binds PI4P and requires PI4P for TGN targeting (Wang *et al.*, 2003; Heldwein *et al.*, 2004). PI4P is particularly enriched at the TGN (Wang *et al.*, 2003), and additional TGN-localized proteins, such as epsinR (Hirst *et al.*, 2003), OSBP (Levine and Munro, 2002), and FAPP (Godi *et al.*, 2004), that bind PI4P have also been identified. Because these TGN-enriched adaptor proteins bind both PI4P and the small GTPase ADP-ribosylation factor 1 (Arf1), we and others proposed that PI4P and Arf1 are essential components of a coincidence detection network that specifies their recruitment to the TGN (Wang *et al.*, 2003; Godi *et al.*, 2004; Behnia and Munro, 2005; Carlton and Cullen, 2005).

This paradigm begs the question of whether the Golgi-localized, γ-ear containing, Arf-binding proteins (GGAs), a major family of TGN-enriched adaptors that mediate trafficking between the TGN and endosomes (Bonifacino, 2004), also use PI4P to ensure organelle-specific targeting. It has been clearly established that GGA association with the TGN is dependent on the small GTPase Arf1 (Puertollano *et al.*, 2001; Takatsu *et al.*, 2002; Collins *et al.*, 2003) and that the Arf1 binding site is located at the NH_2-terminus of the GAT (GGA and Tom1) domain (Shiba *et al.*, 2003; Bilodeau *et al.*, 2004; Kawasaki *et al.*, 2005; Prag *et al.*, 2005). This domain is sandwiched between the VHS (Vps27, Hrs, STAM) and the appendage domains in GGA's linear sequence (see Figure 2A). The VHS domain binds to the acidic cluster-dileucine motifs found on cargo proteins (Doray *et al.*, 2002; Puertollano *et al.*, 2001; see Figure 2A).

Humans have three GGAs (GGA1, GGA2, and GGA3). GGA1 and 3 bind monoubiquitin (Ub) and may therefore sort ubiquitinated cargoes (Bilodeau *et al.*, 2004; Puertollano and Bonifacino, 2004; Scott *et al.*, 2004). *Saccharomyces cerevisiae* has two Gga proteins, called Gga1p and 2p, which also sort ubiquitinated cargo proteins between the TGN and endosomes (Bonifacino, 2004; Scott *et al.*, 2004; Kim *et al.*, 2007). GGAs have two Ub-binding sites that are located downstream of the Arf1-binding site in the GAT domain (Bilodeau *et al.*, 2004; Mattera *et al.*, 2004; Puertollano and Bonifacino, 2004; Shiba *et al.*, 2004; Kawasaki *et al.*, 2005; Prag *et al.*, 2005; see Figure 2, A and B).

In this article, we examine the role of PI4P in the recruitment of the GGAs. We establish that PI4P is essential for

This article was published online ahead of print in *MBC in Press* (http://www.molbiolcell.org/cgi/doi/10.1091/mbc.E06–10–0897) on May 9, 2007.

† These authors contributed equally to this work.

Address correspondence to: Helen L. Yin (Yin@UTSouthwestern.edu).

Abbreviations used: PI4P, phosphatidylinositol 4-phosphate; PI4KIIα, phosphatidylinositol 4-kinase type IIα; TGN, *trans*-Golgi network; GGA, Golgi-localized, γ-ear containing, ADP-ribosylation factor binding protein; GAT, GGA and Tom1 domain; C-GAT, C-terminal GAT; N-GAT, N-terminal GAT; VHS, Vps-27, Hrs, and STAM domain; Arf1, ADP-ribosylation factor 1; Ub, ubiquitin; PS, phosphatidylserine; PC, phosphatidylcholine; PE, phosphatidylethanolamine; ITC, isothermal titration calorimetry.

their TGN recruitment and that PI4P also promotes GGA binding to ubiquitinated cargoes.

MATERIALS AND METHODS

Antibodies and Reagents

Affinity-purified rabbit polyclonal anti-PI4KIIα was generated as described previously (Wei *et al.*, 2002). Other antibodies were obtained as follows. Polyclonal antibodies: sheep anti-TGN46 (Serotec, Raleigh, NC), goat anti-GST (Amersham Pharmacia, Piscataway, NJ), rabbit anti-GGA1 (a gift of M. S. Robinson, University of Cambridge); secondary antibodies (Jackson ImmunoResearch, West Grove, PA; Amersham; or Santa Cruz Biotechnology, Santa Cruz, CA). Monoclonal antibodies: anti-Arf (ABR Affinity Bioreagents, Golden, CO), anti-myc (Santa Cruz), anti-HA (Covance, Princeton, NJ), anti-GGA2, anti-GGA3, and anti-His (BD Transduction Laboratories, Lexington, KY), anti-actin (Sigma, St. Louis, MO). Most of the other reagents were from Sigma, except as noted in the text.

Cell Culture and Plasmid Transfections

HeLa cells were cultured in DMEM with 10% (vol/vol) fetal bovine serum (FBS), 10 mM HEPES, and 1 mM sodium pyruvate at 37°C. They were transiently transfected with plasmid and lipofecAMINE 2000 (Invitrogen, Carlsbad, CA), and cells were processed for immunofluorescence 18–24 h later.

RNA Interference

The PI4KIIα small interfering RNA (siRNA) primers used were as described previously (Wang *et al.*, 2003). HeLa cells were plated in six-well plates at between 30 and 40% confluence for 24 h and transfected with 10 μl of 20 μM siRNA and 3 μl Oligofectamine (Invitrogen) in 1 ml of Opti-MEM. After 5 h, cells were rinsed and cultured in DMEM containing 10% FBS. Cells were fixed at 72 h after the initial siRNA treatment. GGA1 RNA interference (RNAi) and rescue was performed based on the method described by Ghosh *et al.* (2003), except that siRNA oligos (^{463}AAGCTTCCAGATGACACTACC^{483}[AF190862]) were used for knockdown, and transient GGA1 cDNA transfection was used for rescue. The cells were transfected with the GGA1 cDNA 54 h after the initial siRNA transfection and harvested 18 h after cDNA transfection.

Immunofluorescence Microscopy and Image Analyses

In most cases, cells were processed for immunofluorescence microscopy after fixation in 3.7% formaldehyde at room temperature for 15 min followed by permeabilization in 0.1% Triton X-100 on ice for 5 min. In the case of Arf staining, cells were fixed with methanol at −20 C for 10 min. Fixed and permeabilized cells were incubated with antibodies in phosphate-buffered saline (PBS) containing 1% bovine serum albumin (BSA) and 3% donkey serum. Immunofluorescence was detected by a Zeiss LSM510 laser scanning confocal microscope (Thornwood, NY) using a 63× oil 1.3 NA PlanApo objective. The GGA fluorescence intensity ratio of TGN/entire cell was obtained from cells in randomly chosen fields, using the Metamorph software (Universal Imaging, West Chester, PA), as described previously (Wang *et al.*, 2003). The effect of GGA1 RNAi on the TGN morphology was examined by scoring 150–200 cells per condition for the presence of normal compact perinuclear TGN46 staining or abnormally expanded TGN46 staining.

Subcellular Fractionation

HeLa cells were resuspended in lysis buffer (250 mM sucrose, 20 mM Tris-HCl, pH 7.5, 1 mM EDTA, and protease inhibitors) homogenized in a steel Dounce homogenizer with 25 strokes, and the cell lysates were centrifuged at 1000 × *g* for 5 min to remove cell debris and nuclei. The postnuclear supernatants were centrifuged at 100,000 × *g* to obtain the cytosol (sup, S) and membrane fractions (pellets, P).

Generation of GGA Truncated Fragments and GGA Mutants

The GGA2 VHS-GAT pGEX-4T-1 bacterial expression vector used is as described by Collins *et al*. (2003). Truncated GGA2 fragments (VHS, GAT, N-GAT, C-GAT, and GAT α3, α4, and α34) were generated by PCR and subcloned into BamHI-NotI sites of pGEX-4T-1 vector for protein purification or BamHI-SmaI sites of pCMV5/myc1 for overexpression in HeLa cells. Site-directed mutagenesis was performed using the QuickChange kit (Stratagene, La Jolla, CA). PCRs were performed using an overlap extension by *Pfu* Turbo DNA polymerase with full-length GGAs or GAT domain constructs as templates. Mutations were confirmed by nucleotide sequencing analysis.

Protein Expression and Purification

The GGA1 and GGA2 constructs were as described previously (Puertollano *et al.*, 2001; Collins *et al.*, 2003). Truncated GGA fragments (VHS, GAT, N-GAT, C-GAT, and GAT α3, α4, and α34) were generated by PCR and subcloned into BamHI-NotI sites of pGEX-4T-1 vector for protein purification or BamHI-SmaI sites of pCMV5/myc1 for overexpression in HeLa cells. Site-directed mutagenesis was performed using the QuickChange kit (Stratagene). Mutations were confirmed by nucleotide sequencing. The GST-tagged fusion proteins were expressed in the *Escherichia coli* strain BL21 (Invitrogen) using isopropyl-1-thio-β-D-galactopyranoside (IPTG) induction at 20°C. Recombinant GGA domains were collected on glutathione Sepharose 4 Fast Flow (Amersham Biosciences) and eluted with glutathione elution buffer containing 10 mM reduced glutathione and 50 mM Tris HCl (pH 8.0). Myr-Arf1 was expressed in *Escherichia coli* cotransformed with full-length Arf1 and *N*-myristoyl transferase (Duronio *et al.*, 1990; Franco *et al.*, 1995; Heldwein *et al.*, 2004). Myr-Arf1 was purified as described (Duronio *et al.*, 1990; Franco *et al.*, 1995), and charged with GTP by incubating it (at 10 μM) with 100 μM GTPγS in 20 mM Tris, pH 7.5, 100 mM $MgCl_2$, 2 mM EDTA, 1 mM DTT for 45 min at 37°C. The reaction was stopped by adding 2 mM $MgCl_2$. Purified recombinant His-monoubiquitin (His-Ub) was a gift of G. DeMartino (UT Southwestern) and bovine Ub was purchased from Sigma. The yeast Gga1p His-VHS-GAT was expressed in *Rosetta* cells (Novagen, Madison, WI) using standard protocols with IPTG induction at 30°C. Recombinant proteins were affinity purified on nickel nitrilotriacetic acid His-Bind Resin (Novagen) in Tris-buffered saline (TBS; 10 mM Tris, 140 mM NaCl, pH 8.0) with 5 mM imidazole and eluted with TBS with150 mM imidazole.

Liposome Pulldown Assay

All lipids were from Sigma, unless otherwise specified. Mixed lipid vesicles containing 57% dioleoyl phosphatidylcholine (PC), 28% dipalmitoyl phosphatidyl-ethanolamine (PE), and 15% of either phosphatidylserine (PS), PI4P (Avanti Polar Lipids, Alabaster, AL), PI3P (Echelon Biosciences, Salt Lake City, UT), or PI(4,5)P2 (Echelon Biosciences) were prepared (Heldwein *et al.*, 2004). Lipids were dissolved in chloroform and mixed in the appropriate ratio. Chlorofom was evaporated under a slow stream of nitrogen, and the dried lipids were resuspended in cyclohexane and immediately placed in dry ice. The frozen mixture was dried in a lyophilizer, and the resulting dry powder was resuspended in TBS (10 mM Tris·HCl, pH 7.5, 50 mM NaCl, 1 mM dithiothreitol [DTT]) to 5 mg/ml by vortexing vigorously at room temperature to obtain a milky suspension. In most studies, 0.02 mg/ml recombinant GGA fragments were incubated with 0.2 mg/ml lipid vesicles for 15 min at room temperature in a final volume of 75 μl in TBS. Liposomes were collected by centrifugation at 200,000 × *g* for 10 min, and after carefully removing the supernatant, the pelleted protein was dissolved in gel sample buffer. GGA domain proteins in the supernatants and pellets were stained by Coomassie blue after SDS-PAGE and quantitated by densitometry.

Protein-Lipid Overlay Assay

Recombinant GST-tagged GGA domains, His-tagged yeast Gga domains or His-tagged Ub was incubated with PIP-Arrays (Echelon Biosciences) or homemade lipid strips at 4°C overnight as described previously (Wang *et al.*, 2003). "Homemade" lipid strips were prepared by spotting serially diluted phosphoinositides (100, 50, and 25 pmol, from Echelon Biosciences) on Hybond-C extra nitrocellulose membrane (Amersham). Membranes were washed extensively with TBS containing 0.1% (vol/vol) Tween and probed sequentially with primary antibodies and horseradish peroxidase–conjugated secondary antibodies. Bound immunocomplexes were identified with ECL Plus (Amersham) and quantitated using the Storm phosphorimager (GE Healthcare, Waukesha, WI).

Ub-Agarose Binding Assay

GGA GST-GAT or Gga1p His-VHS-GAT, both 0.5 μM, was incubated with PI4P micelles for 15 min at room temperature in buffer A (25 mM HEPES, pH 7.4, 125 mM KOAc, 2.5 mM MgOAc, 5 mM EGTA, and 1 mM DTT) in a 100 μl volume. Ub- or protein A-agarose beads, both 15 μl, that were precoated with 0.1% BSA were added. After 60 min, the beads were pelleted at 1000 × *g* and washed five times with buffer A containing 1% Triton X-100. Bound GST-GAT or yeast Gga1p His-VHS-GAT was detected by Western blotting with anti-GST or anti-His antibody, respectively.

In Vivo Ubiquitination

HeLa cells were cotransfected with myc-GGA1 and hemagglutinin (HA)-Ub cDNA (a gift from K. Orth, UT Southwestern) as described (Shiba *et al.*, 2004). Myc-GGA1 was immunoprecipitated with anti-myc antibody, and ubiquitinated GGA1 was detected by Western blotting with anti-HA. The extent of ubiquitination of the immunoprecipitated GGA1 was expressed as a ratio of the intensity of the HA-Ub and myc-GGA1 in the Western blot.

Isothermal Titration Calorimetry

GGA1 GST-GAT1 and bovine Ub were dialyzed against PBS supplemented with 2 mM β-mercaptoethanol. Protein concentrations were determined using the extinction coefficients of 50, 900, and 1280 M^{-1} cm^{-1} for GST-GAT and Ub, respectively. GST-GAT was placed in the sample cell of a Microcal VP isothermal titration calorimetry (ITC) instrument at 50 μM and Ub (0.5 mM

initial concentration) was injected serially into the reaction chamber at 30°C. When appropriate, 50 μM water-soluble PI4P (diC8PI4P, Echelon Biosciences) was incubated with GST-GAT1 and His-Ub separately at 30°C, before injection. Data were fitted by using the ORIGIN software (OriginLab, Northampton, MA).

RESULTS

GGAs' TGN Targeting Is PI4P Dependent

To determine if PI4P is important for the recruitment of the GGAs to the TGN, we used RNAi to knockdown phosphatidylinositol 4 phosphate kinase IIα (PI4KIIα), a resident TGN protein that generates the bulk of the TGN's PI4P (Barylko *et al.*, 2001; Wang *et al.*, 2003). In the absence of RNAi treatment, all three mammalian GGAs were concentrated at the TGN, which was identified by staining with anti-TGN46 (Figure 1, A–C, left panels). PI4KIIα depletion decreased the association of all three GGAs with the TGN (Figure 1, A–C, right panels), and induced redistribution of GGAs to punctuate and/or tubular endomembranes, as well as to the cytoplasm. GGA1 had the most particulate extra-Golgi staining, suggesting that it might associate with membranes somewhat better than GGA2 and 3 even in the absence of PI4P. The immunofluorescence images were used to estimate the extent of TGN association. The fluorescence intensity of the GGAs per unit area in the TGN was expressed relative to that for the entire cell to obtain a TGN "intensity ratio." The intensity ratios for GGA1 in control and PI4KIIα RNAi cells are 9.57 ± 0.48 (n = 10) and 2.67 ± 0.16 (n = 10), respectively. Thus, there was a 72% decrease in the association of GGA1 with the TGN in the cells treated with PI4KIIα siRNA.

We also used biochemical fractionation to determine if PI4KIIα depletion altered the association of GGA1 with membranes. PI4KIIα RNAi decreased GGA1 association with the membrane pellet by 40 ± 7% (n = 3) and increased the amount recovered in the supernatant (Figure 1A, Western blot). In contrast, the partitioning of β-COP, a Golgi-enriched protein that does not bind PI4P, was not changed at all. Therefore, PI4KIIα depletion blocked GGA1 recruitment specifically. The 40% decrease in membrane association estimated by fractionation is less than the 72% decrease in TGN association estimated by immunofluorescence staining and is consistent with the fluorescence images showing that some GGA1 redistributed to extra-Golgi membranes after PI4KIIα depletion.

GGAs require Arf1-GTP for TGN localization (Puertollano *et al.*, 2001; Takatsu *et al.*, 2002; Collins *et al.*, 2003). Therefore, we investigated the possibility that GGAs mislocalization in PI4KIIα RNAi-treated cells is secondary to a disruption of Arf1 activation. PI4KIIα RNAi had little effect on Arf1 localization in the perinuclear region of the cells (Figure 1D), as the intensity ratios for Arf in control and PI4KIIα RNAi cells are 3.00 ± 0.10 (n = 10) and 2.84 ± 0.14 (n = 9), respectively. Because only activated Arf1 binds the Golgi and TGN, PI4KIIα RNAi disrupts GGAs' TGN targeting primarily by depleting PI4P and not by severely compromising Arf1 activation.

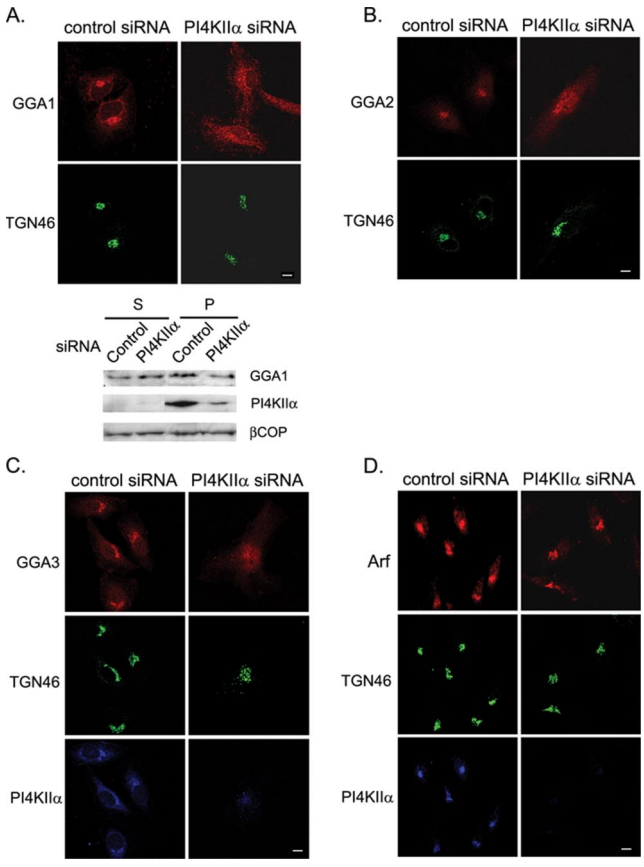

Figure 1. Effects of PI4KIIα RNAi on the intracellular distribution of the GGAs and Arf in cells. (A–C) Effects on GGA localization. Endogenous GGA1, 2, and 3 were detected with isoform-specific antibodies. The TGN was stained with anti-TGN46. Western blot in A shows the partitioning of GGA1, PI4KIIα, and βCOP in the 100,000 × *g* supernatants (S) and pellets (P). Densitometry scanning showed that there was a 40 ± 7% (n = 3) decrease in membrane-associated GGA1 in the PI4KIIα-RNAi–treated cells. (D) Effects on Arf localization. The anti-Arf antibody recognizes all Arfs, but Arf1 is the most abundant and it is concentrated in the Golgi apparatus. Scale bar, 20 μm.

GGA Binds PI4P Primarily through Its GAT Domain

To identify the mechanism by which PI4P recruits GGAs to the TGN, we first determined if the GGA domains bind PI4P directly. Recombinant GST-GGA2 VHS-GAT, GAT, and VHS were incubated with mixed lipid vesicles containing either PI4P or PS. All three constructs bound PI4P, but GAT bound the most. In the gel shown in Figure 2C, 93% of GAT sedimented with the PI4P liposomes, whereas 42% VHS-GAT and 50% VHS sedimented. These results suggest that the GAT domain bound PI4P much more strongly than VHS, but that VHS inhibited binding of GAT to PI4P in VHS-GAT. Previous studies have shown that although VHS and GAT can function as independent modules, they can alter the binding of each other to select ligands when expressed in tandem (Hirsch *et al.*, 2003; Mattera *et al.*, 2004).

Binding was not simply due to charge–charge interactions, because only 10% of GAT sedimented with liposomes containing another basic lipid, PS (Figure 2C, SDS gel). The ratio of binding to PI4P versus PS liposomes from several experiments was calculated and is referred to as PI4P binding index in the bar graph shown in Figure 2C. GGA2 GAT binds PI4P liposome 6.8 ± 0.5 (mean ± SE, n = 5) times better than PS liposome, whereas VHS-GAT and VHS bound 3.3 ± 0.4 (n = 5) and 2.9 ± 0.5 (n = 6), respectively. Like GGA2 GAT, GGA1 GAT also bound PI4P mixed lipid vesicles in a dose-dependent manner, and there was no obvious difference between them (Figure 2D).

The preference of GAT for PI4P was confirmed by lipid dot blot assays. GGA2 GAT bound PI4P preferentially compared with other mono-, di-, or triphosphorylated phosphoinositides (Figure 2D). In agreement with the liposome pull-down assays, VHS did not bind PI4P as well as GAT. We

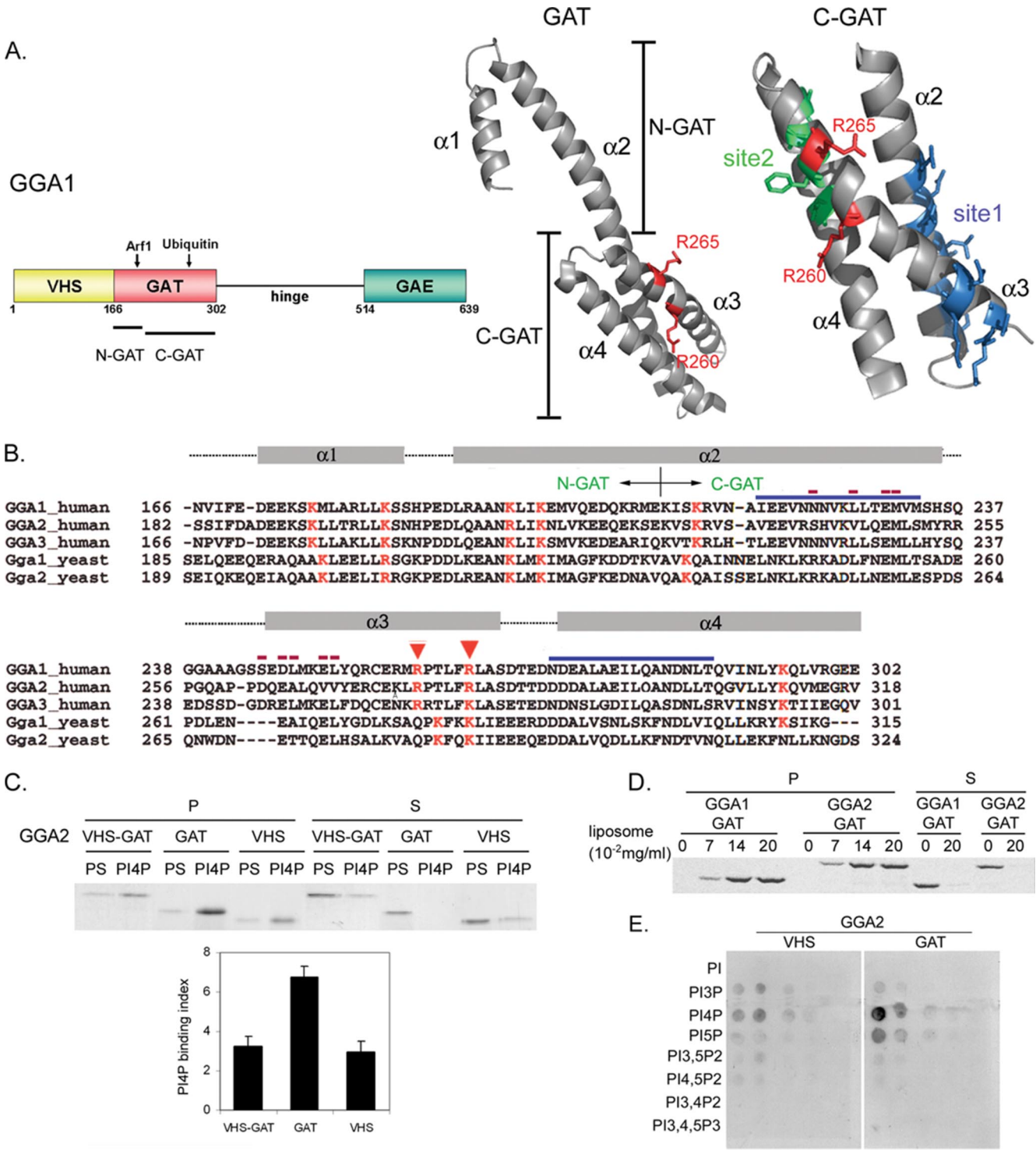

Figure 2. GGA GAT binding to PI4P. (A) GGA domain organization and structure. Left, the modular organization of the GGA domains. The GGA1 domain boundaries are as defined by Suer *et al.* (2003). The GAT domain is further divided into the N-GAT and C-GAT domains, which bind Arf1 and Ub, respectively. Our data showed that C-GAT also binds PI4P. Middle, a ribbon diagram of the X-ray crystal structure of GGA1 GAT, adapted from Collins *et al.* (2003). The GAT domain has four helices (named α1–4). The N-GAT domain has a hook-helix (α1 and part of α2), and the C-GAT domain has a three-helix bundle that is comprised of a portion of α2 and the entire α3 and α4. The PI4P-binding residues, GGA1 R260 and R265 (equivalent to GGA2 R276 and R281) are highlighted in red. We showed the GGA1 GAT structure instead of the GGA2 GAT structure here because only the former has been solved at the atomic level. Right, an expanded view of the GGA1 C-GAT structure. The C-GAT domain is rotated slightly in order to display the relation between the Ub-binding sites and PI4P-binding residues. Red, PI4P-binding residues; blue and green, Ub-binding residues in sites 1 and 2, as defined in yeast (Bilodeau *et al.*, 2004). Additional site 1 residues identified by X-ray crystallography of the mammalian GGA GAT:Ub (Bilodeau *et al.*, 2004; Kawasaki *et al.*, 2005; Prag *et al.*, 2005) that fall outside of these regions are not highlighted to simplify the presentation (see panel B). The site 1 residues were observed to bind Ub in the GGA3 GAT:Ub structure by Prag *et al.* (2005) and Kawasaki *et al.* (2005). The site 2 binding residues were identified

therefore focused on identifying the minimal PI4P-binding domain in GAT.

Identification of GAT's Minimal PI4P-binding Domain

The GAT domain has multiple binding partners. It binds Arf1-GTP through the NH_2-terminal "hook" region (referred to as N-GAT; Collins *et al.*, 2003; Suer *et al.*, 2003; see Figure 2, A and B, for definition). It also binds Ub and Rabaptin 5 at its COOH-terminal triple helix bundle (C-GAT), which encompasses the C-terminal half of helix α2 and helices α3 and α4 (Bilodeau *et al.*, 2004; Mattera *et al.*, 2004; Kawasaki *et al.*, 2005; Prag *et al.*, 2005). The C-GAT domain bound PI4P in lipid dot blots (Figure 3A), whereas the N-GAT domain did not (data not shown). The GAT α3 + α4 helices together bound PI4P much better than either α3 or α4 individually (Figure 3A). Therefore, it is likely that the GGAs bind PI4P through their GAT α3 and α4 helices.

Identification of the GAT PI4P-binding Site

Site-directed mutagenesis was used to identify the residues in these helices that are essential for PI4P binding. Phosphoinositides bind proteins through multiple interactions, including contacts between their negatively charged phosphate head groups and the side chains of basic amino acid residues (Yin and Janmey, 2003). GGA GAT α3 and α4 do not have obvious sequence or structural similarity to any of the known PI4P-binding motifs (Mao *et al.*, 2001; Levine and Munro, 2002; Collins *et al.*, 2003; Hirst *et al.*, 2003; Godi *et al.*, 2004; Heldwein *et al.*, 2004; Yu *et al.*, 2004). However, they have three highly conserved solvent exposed basic residues (GGA2 R276, R281, and Y310) that can potentially interact with PI4P's phosphate groups (Figure 2, A and B; equivalent to GGA1 R260, R265, and Y294). These residues were mutated individually to glutamic acid (E) or alanine (A) for in vitro or in vivo studies.

In liposome pulldown assays, 89% of wild-type (wt) GAT sedimented with PI4P liposomes, whereas much less sedimented with liposomes containing other acidic lipids (Figure 3B). In contrast considerably less GAT R276E, R281E, and Y310E cosedimented with PI4P liposomes, and there was no significant difference in the amount bound to other acidic lipids (Figure 3B). These results suggest that these three basic residues may be essential for PI4P binding in vitro.

Although GGA2 R276, R281, and Y310 are far removed from the N-GAT region that binds Arf1 (Figure 2A), it is nonetheless important to evaluate the effect of their mutation on Arf1 binding. We adopted a PS liposome pulldown method that was used previously to show that Arf1-GTP promotes binding of the clathrin adaptor AP-1 complex to lipid vesicles (Heldwein *et al.*, 2004). GGA2 GAT bound PS containing vesicles, and binding was increased by 2.2-fold by Arf1-GTP. Arf1-GTP also increased GGA2 GAT R276E and R281E binding to PS vesicles by a statistically significant extent (Figure 3C). Therefore, these mutations selectively impaired PI4P binding without affecting the ability of the GAT domain to interact with Arf1-GTP. Therefore, GGA2 R276 and R281 are important for PI4P binding in vitro. Both residues are conserved in the human GGAs and yeast Gga proteins (Figure 2B), which also bind PI4P (see Figure 5C).

In contrast, the GGA2 GAT Y310 mutation decreased PI4P binding (Figure 3B) and compromised the ability of Arf1 to promote GAT binding to liposomes (Figure 3C). These results suggest that the Y310E mutation may have changed the conformation of GAT, as would be consistent with the previous suggestion that Y310 contributes to the packing of the α2+α3+α4 three helix bundle (Shiba *et al.*, 2004). In view of this change, we cannot conclude based on the current data that Y310 contributes to PI4P interaction.

PI4P-binding Site Mutants Have Decreased Association with the TGN

The GGA2 GAT PI4P binding mutants were expressed in cells to assess the impact of decreased PI4P binding on GAT recruitment to the TGN. As shown previously, the wt GAT domain was targeted to the TGN (Puertollano *et al.*, 2001; Takatsu *et al.*, 2002; Collins *et al.*, 2003; Figure 4A). In contrast, GGA2 GAT R276E, R281E, and R281A were not TGN associated, even when expressed at low levels (e.g., see arrows in the R281A panel of Figure 4A). The expressed mutants were predominantly cytosolic, although some were also present in the nucleus. The intensity ratio in the TGN relative to the entire cell was 1.54 ± 0.07 ($n = 10$) for GGA2 GAT R276E compared with 4.79 ± 0.38 ($n = 10$) for wt GAT. GAT K311E, which bound PI4P normally in vitro (data not shown), was still enriched in the TGN (Figure 4A), with an intensity ratio of 3.64 ± 0.2 ($n = 11$). The strong correlation between the ability of the GAT domain to bind PI4P in vitro and to associate with the TGN in vivo establishes that the recruitment of the GAT domain to the TGN requires PI4P.

We also examined the behavior of the PI4P binding mutations in the context of the full-length GGAs. GGA2 R276A and R281A were mostly cytosolic (Figure 4B), confirming that these residues are important for TGN targeting of the full-length protein. Unlike the equivalent GATs (Figure 4A), they were not nuclear localized, and they were slightly more TGN associated. Overall, these results demonstrate that PI4P binding is essential for the TGN localization of the GGAs and that the other interactions mediated by the modules outside of the GAT domain are not sufficient to recruit the GGAs to the TGN in the absence of PI4P binding.

The decrease in mutant GGAs association with membrane was confirmed biochemically. High-speed centrifugation pelleted 10.4% of wt GGA2, but only 1.0 and 2.4% of GGA2 R276A and R281A, respectively (Figure 4B, right panel).

Figure 2 (cont). by site-directed mutagenesis (Bilodeau *et al.*, 2004; Puertollano and Bonifacino, 2004; Shiba *et al.*, 2004). (B) Sequence alignment of the human and yeast GAT domains. Rectangles, helices in GAT; dotted lines, linkers between helices. The boundaries used to generate the N-GAT and C-GAT are indicated. Red letters denote basic amino acids that were conserved among different species. GGA1 R260 and R265 are conserved in mammalian and yeast GGAs, except that there is a two-residue offset in the yeast proteins. Red arrowheads, PI4P binding residues identified in this study. Blue lines, Ub-binding sites 1 and 2 that were identified in yeast (Bilodeau *et al.*, 2004). Red lines, site 1 residues observed to bind Ub in GGA3 GAT:Ub crystals (Kawasaki *et al.*, 2005; Prag *et al.*, 2005). There is currently no crystal structure of GAT site 2 bound to Ub. The mammalian site 2 residues identified by site-directed mutagenesis (Bilodeau *et al.*, 2004; Puertollano and Bonifacino, 2004; Shiba *et al.*, 2004) are not highlighted here. (C) Comparing the binding of GGA2 domains to liposomes. 0.02 mg/ml purified GGA2 GST-VHS-GAT, GAT, and VHS were incubated with 0.2 mg/ml mixed lipid vesicles containing 15% PS or PI4P. The liposomes were collected by centrifugation and the bound GGA proteins were detected by Coomassie blue staining. The bottom panel shows the ratios of protein cosedimentated with PI4P versus PS liposomes (PI4P-binding index; mean ± SE, n = 5 or 6). (D) Comparing the binding of GGA1 and GGA2 GAT to PI4P-containing liposomes. GAT proteins (0.02 mg/ml) were incubated with increasing amount of liposomes. (E) Comparing the binding of GGA2 VHS and GAT domains to lipid dots. Proteins were incubated with PIP-arrays (Echelon, dotted with lipids ranging from 100 to 1.6 pmol), and the bound GGA domains were detected with anti-GST antibody.

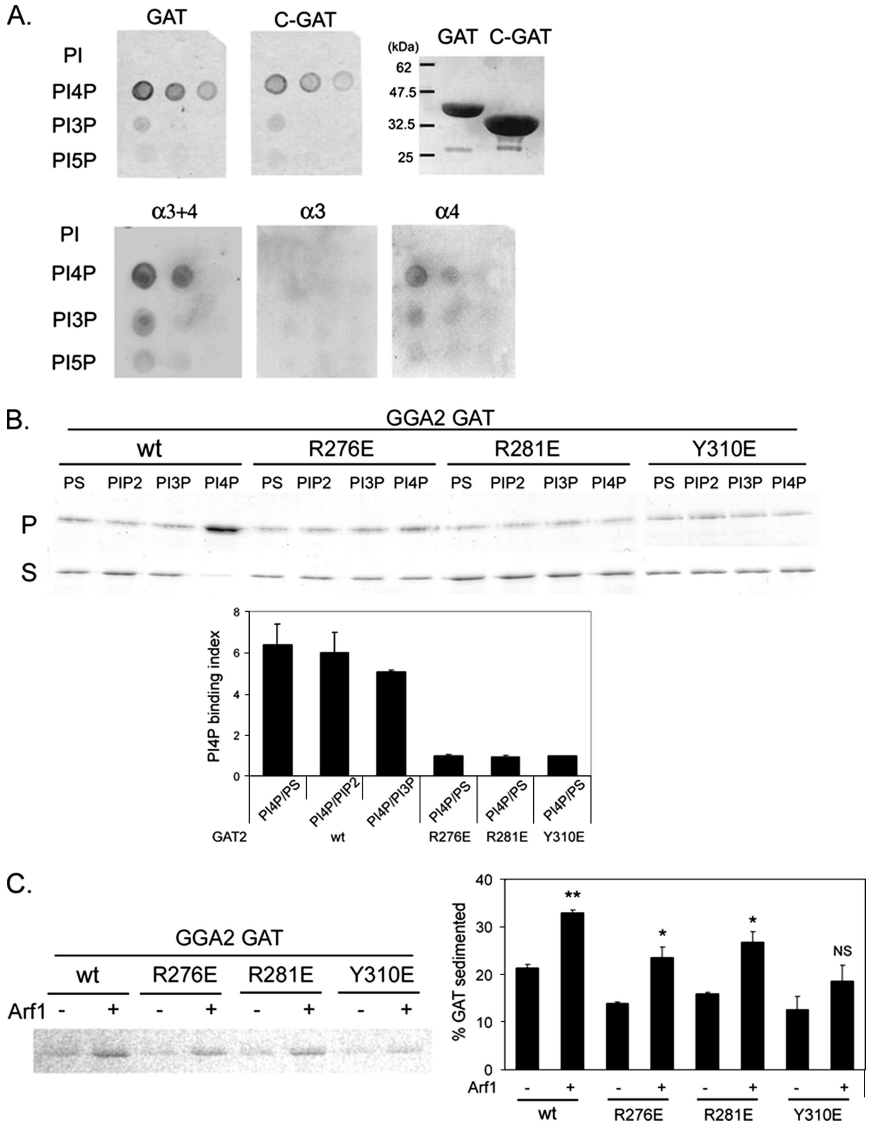

Figure 3. Identification of the GAT PI4P-binding site. (A) Recombinant GGA GST-GAT and its subdomains were incubated with nitrocellulose membranes dotted with 100, 50, and 25 pmol lipids. These lipid dot blots were made in the laboratory. A Coomassie blue–stained gel of the recombinant GST-GAT and GST-C-GAT used is shown. (B) Comparing the binding of wt and mutant GGA2 GAT to liposomes. 0.02 mg/ml (0.4 μM) GGA2 GST-GAT was incubated with 0.2 mg/ml mixed lipid vesicles. The vesicles were sedimented by centrifugation and bound proteins were detected by Coomassie blue staining after SDS-PAGE. The bottom panel shows the ratios of protein cosedimentated with PI4P versus PS liposomes (PI4P-binding index), as mean ± SE from two to four experiments. (C) Comparing the effect of Arf1-GTP on GAT binding to PS liposomes. PS liposomes were preloaded with or without recombinant myr-Arf1-GTPγS. The percent of GAT sedimented was shown in the right panel (mean ± SE, n = 3). **p = 0.003, *p = 0.02, NS (not significant), p = 0.15.

The GGA PI4P-binding Mutant Is Functionally Defective in Cells

To address the question of whether these PI4P binding mutations rendered the GGAs functionally defective, we used a GGA1 RNAi rescue protocol as a readout (Ghosh *et al.*, 2003). After GGA1 was depleted by RNAi, the cDNA for wt and mutant GGAs were introduced to determine if they can rescue the knockdown phenotype. Normally, HeLa cells had a compact TGN, and only 12% of the control (mock) siRNA-transfected cells had an expanded TGN phenotype (Figure 4C). As shown previously (Ghosh *et al.*, 2003), GGA1 depletion increased the percentage of cells with abnormally expanded TGN to 50%. This abnormal phenotype was rescued by overexpressing GGA1, as evidenced by the drop in the percentage of cells with expanded TGN back to 8% (Figure 4C). GGA1 R260A (which is equivalent to the GGA2 R276A) was not targeted to the TGN, and, significantly, it was not able to rescue the expanded TGN phenotype (42% abnormal TGN) of GGA1-depleted cells (Figure 4C). Similar results were obtained with the GGA1 R265A mutant (equivalent to GGA2 R281A, data not shown). Therefore, these PI4P binding mutants are functionally defective in the in vivo context.

GGA's TGN Targeting Has a Dual Requirement for PI4P and Arf1

Because PI4P binding is necessary for GGA's TGN recruitment and function in cells, we asked if PI4P binding per se is sufficient for the GGAs' TGN localization. We also reexamine the notion that Arf1 binding is sufficient for GAT targeting (Collins *et al.*, 2003). This model was based on an in vitro recruitment assay in which N-GAT, which binds Arf1 but not PI4P, was added to permeabilized cells in the presence of cytosol and GTPγS (Collins *et al.*, 2003). Neither GGA2 C-GAT, which binds PI4P but not Arf1, nor GGA2 N-GAT domain, which binds Arf1 but not PI4P, was concentrated in the perinuclear region (Figure 4D). The fluorescence intensity ratios of TGN/entire cell for GAT, C-GAT, and N-GAT were 4.8 ± 0.4 (n = 10), 2.1 ± 0.1 (n = 13), and 1.8 ± 0.1 (n = 8), respectively. The 56 and 62% decrease in TGN association by C-GAT and N-GAT, respectively, showed that neither PI4P binding nor Arf1 binding alone was sufficient for TGN recruitment. Because TGN recruitment requires both N- and C-GAT, we conclude that the is a dual requirement for both Arf1 and PI4P interaction for the proper localization of GGAs at the TGN.

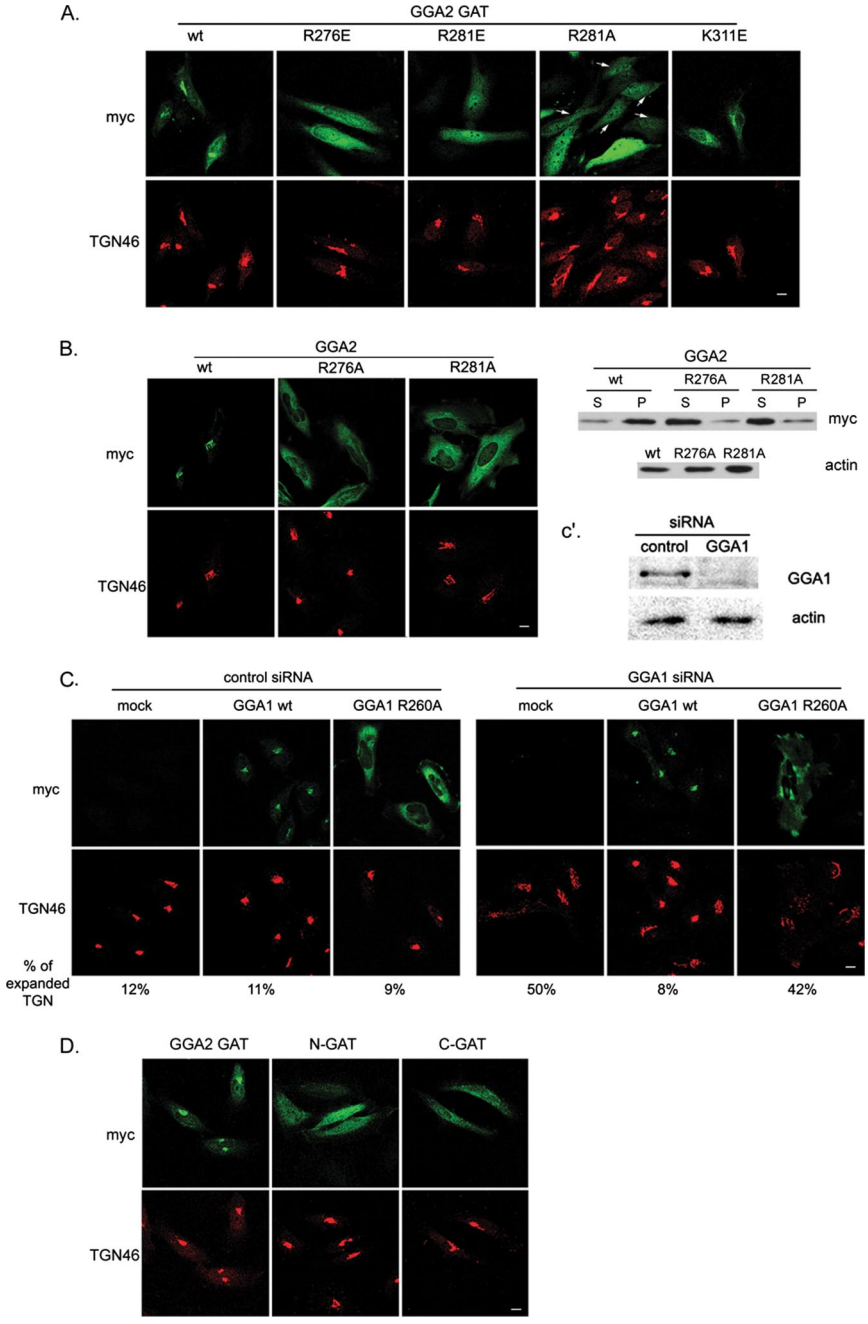

Figure 4. The requirements for GGA targeting to the TGN. (A) GAT targeting. Cells were transfected with myc-tagged GGA2 GAT wt or mutant cDNA. Arrows indicate cells overexpressing low amounts of GAT R281A. (B) Full-length GGA2 targeting. Cells were transfected with myc-tagged wt or mutant GGA2 cDNA. Left panels, immunofluorescence staining. Right panels, membrane fractionation, as described in *Materials and Methods*. Supernatant (S) and membrane pellets (P) were analyzed by Western blotting with myc and actin antibodies. (C) GGA1 RNAi rescue. Cells were initially transfected with control or GGA1 siRNA and then subsequently retransfected with either a myc-tagged empty vector (mock), the wt myc-GGA1 or myc-GGA1 R260A cDNA. GGA1 depletion was confirmed by Western blotting in C′. Actin was included as a loading control. The percentage of cells with the expanded TGN46 phenotype is indicated. Data were from a typical experiment and similar results were obtained in three independent experiments. (D) The GGA2 N-GAT and C-GAT domains were less enriched in the TGN than the GAT domain. Scale bar, 20 μm.

PI4P Promotes GAT Binding to Ub

We examined the effect of PI4P on the binding of the GAT domain to Ub. The rationale for these studies is as follows: first, PI4P and Ub both bind to the C-GAT domain (Kawasaki *et al.*, 2005; Prag *et al.*, 2005; Figure 2, A and B), but the extent of their overlap is unknown, and it is not possible to predict a priori whether the overlap would inhibit or promote these ligands' interaction with the GAT domain; second, one of the PI4P-binding residues (GGA1 R260/GGA2 R276) may also be involved in binding to Ub, because its mutation decreased GAT binding to the Ub-agarose (Bilodeau *et al.*, 2004; Mattera *et al.*, 2004; Puertollano and Bonifacino, 2004; Shiba *et al.*, 2004; Kawasaki *et al.*, 2005; Prag *et al.*, 2005). Third, GGA2 GAT binds Ub-agarose more weakly than the other GGAs (Puertollano and Bonifacino, 2004; Shiba *et al.*, 2004), even though its amino acid sequence in the Ub-binding regions is highly homologous to that of the GAT domains of the other GGAs (Figure 2B). This difference raised the possibility that there may be isoform-specific preference for ubiquitin versus nonubiquitin sorting signals.

PI4P micelles promoted GGA1 binding to Ub-agarose in a dose-dependent manner (Figure 5A, left panel). PI4P, 20 μM, increased GGA1 GAT binding to Ub-agarose by 3.7 $\pm$ 0.8-fold (n = 3), and this increase is statistically significant (Figure 5B, left and middle). In contrast, PI3P, which has the same charge as PI4P, did not produce a statistically significant change (Figure 5B, left and middle). PI4P-containing mixed lipid vesicles also promoted Ub binding, whereas PS-containing liposomes did not (Figure 5B, right). GGA2

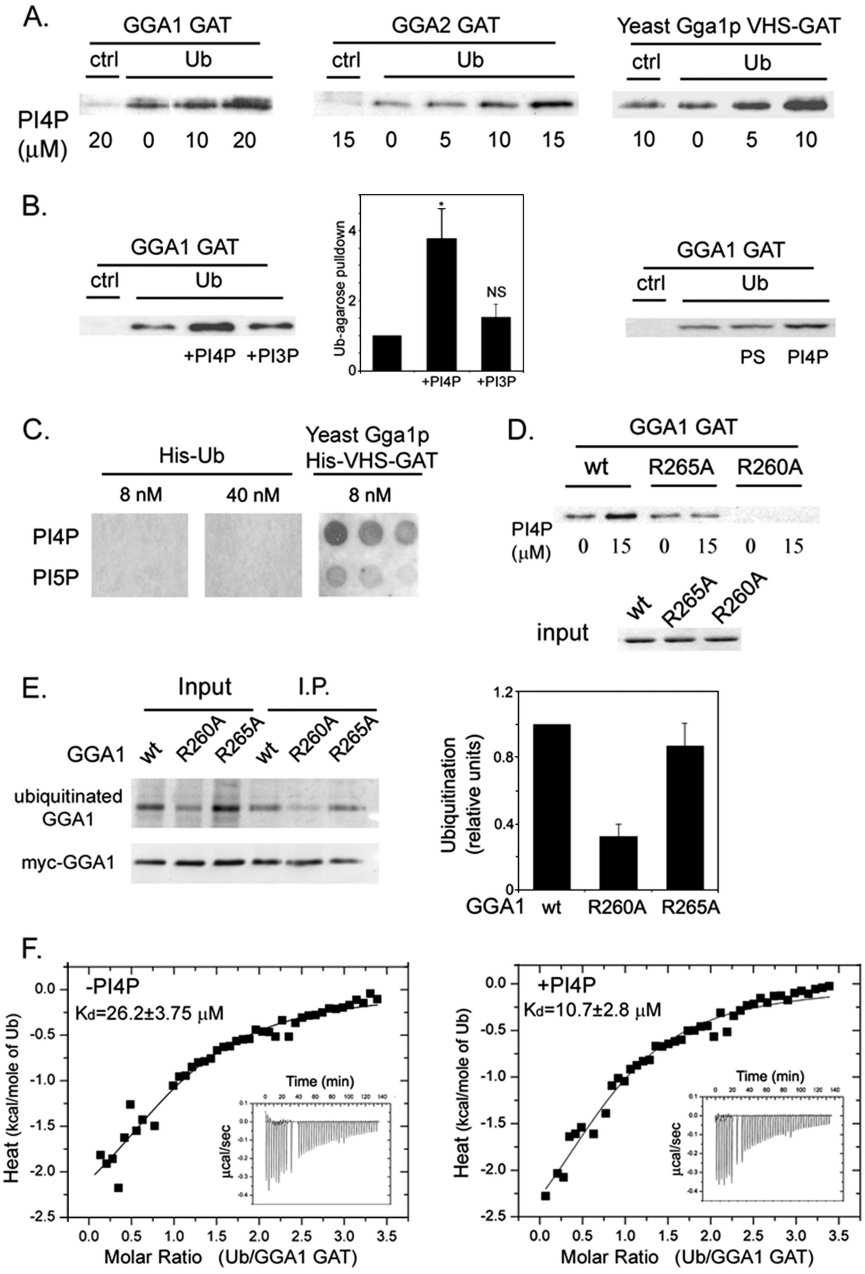

Figure 5. PI4P promotes GAT binding to Ub. (A) Ub-agarose binding. Mammalian GST-GAT or yeast His-VHS-GAT, 0.5 μM, was incubated with increasing amounts of PI4P in the presence of either protein A-agarose (Ctrl) or Ub-agarose. Bound proteins were detected with antibodies by Western blotting. (B) GAT binding to Ub-agarose was preferentially increased by PI4P. GST GGA1 GAT, 0.5 μM, was incubated with 20 μM PI4P or PI3P (left and middle panels) or with PC/PE liposomes containing either PS or PI4P (right panel). PI4P increased GGA1 GAT binding to Ub by 3.73 ± 0.8-fold and PI3P 1.5 ± 0.3-fold (n = 3). *p = 0.024. NS, p = 0.775. (C) His-Ub did not bind PI4P on lipid dot blots. His-Ub (at 8 or 40 nM) and His-VHS-GAT from yeast Gga1p (at 8 nM) were incubated with lipid dots made in the laboratory (lipids: 100, 50, and 25 pmol), and bound proteins were detected with anti-His antibody. (D) PI4P did not promote mutant GAT binding to Ub-agarose. GGA1 GAT wt, R265A, and R260A (0.25 μM) were incubated with Ub-agarose in the presence of 15 μM PI4P. The proteins used for the binding studies are shown (input). (E) GGA1 ubiquitination in vivo. HeLa cells were cotransfected with myc-tagged wt or mutant GGA1 and HA-Ub cDNAs. Myc-GGA1 was immunoprecipitated and blotted with anti-myc antibody to detect GGA1 and anti-HA to detect Ub associated with GGA1. The extent of ubiquitination for each sample was expressed as a ratio of the intensity of the HA-Ub to myc-GGA1 signals in the myc-GGA1 immunoprecipitates, and the value for the wt GGA1 is defined as 1.0. Data shown are mean ± SE (n = 3). (F) ITC analysis. GGA1 GST-GAT and bovine Ub were each preincubated with 50 μM water-soluble diC8PI4P before mixing. The kcal/mol of Ub as a function of the molar ratio of Ub to GGA1 GAT is shown, and the curves were fitted by using a one-site model. The K_d values shown are mean ± SE of five experiments using several different preparations of GGA1 GAT. The insets show the heat change elicited by successive injections of Ub into a chamber containing the GAT1 solution.

GAT, which bound Ub-agarose more weakly than GGA1 GAT, was also stimulated to bind Ub by PI4P (Figure 5A, middle). PI4P, which binds yeast Gga1p His-VHS-GAT directly on lipid dot blots (Figure 5C), also stimulated its binding to Ub-agarose (Figure 5A, right).

Additional experiments establish that the PI4P effect is mediated through GAT binding to Ub. First, His-Ub did not bind PI4P on lipid dot blots, even at a fivefold higher concentration than the yeast Gga1p His-VHS-GAT domain (Figure 5C). Second, GGA1 GAT R265A, which bound Ub-agarose (Figure 5D), did not respond to PI4P. We were not able to use GGA1 GAT R260E for this purpose, because it did not bind Ub-agarose (Figure 5D; Shiba *et al.*, 2004). The difference in the ability of these two PI4P mutants to bind Ub correlates with their ubiquitination (Figure 5E; Shiba *et al.*, 2004).

The effect of PI4P on the interaction between the GAT domain and Ub was examined more quantitatively under true in-solution conditions by ITC. GGA1 GAT binding to Ub released heat (Figure 5F), and the binding isotherm fitted a one-site model that had an estimated K_d value of 26 ± 3 μM (n = 5; Figure 5F). Significantly, in the presence of diC8PI4P, the K_d value for GGA1 GAT:Ub binding decreased by 2.6-fold.

DISCUSSION

The findings presented here establish that GGA1 and GGA2 GAT both bind PI4P in vitro, and the association of all three mammalian GGAs with the TGN is PI4P dependent in vivo. PI4P and Arf1 are both necessary, and importantly, neither alone is sufficient for TGN targeting. Together with other's

findings on epsinR (Hirst *et al.*, 2003), OSBP (Levine and Munro, 2002), and FAPP (Godi *et al.*, 2004), we propose that PI4P is a major lipid platform for the recruitment of almost all of the currently known TGN-enriched clathrin adaptors. Although these adaptors have low estimated affinity for PI4P, their dual requirement for PI4P and Arf1-GTP allows them to act as sensitive coincidence detectors that associate with the TGN in a spatially and temporally appropriate manner (Carlton and Cullen, 2005).

GGAs bind PI4P primarily through their GAT domain. A comparison of the binding data suggests that the VHS domain may also bind PI4P, but to a lesser extent, and that VHS decreases GAT binding to PI4P in VHS-GAT. This finding is unexpected because it has been shown previously that GGA1 VHS-GAT has four times higher affinity for Arf1 than GAT1 alone (Hirsch *et al.*, 2003). Our data here would suggest that VHS regulates Arf1 and PI4P binding in opposite directions. The significance of this difference in the context of the full-length GGA protein remains to be determined. Irregardless of whether PI4P binding by GAT is regulated by VHS, our result clearly demonstrates that GAT is important for GGA recruitment to the TGN. Mutations in the GAT domain show that two conserved basic residues in C-GAT are critical for PI4P binding in vitro (Figure 3B) for association of the full-length GGA with the TGN (Figure 4B) and for maintenance of TGN functions in vivo (Figure 4C). These residues are located in α3 of GAT's three helix bundle (Figure 2, A and B). Mutation of either residue individually diminishes PI4P binding in vitro and TGN recruitment and function in vivo.

The structures of GGA1 GAT alone (Collins *et al.*, 2003) show that GGA1 R260 and R265 are located on the solvent exposed face of the GAT three helix bundle (Figure 2A) and are therefore accessible to the charged phosphate headgroups on PI4P. However, they are separated by 13.7 Å, which is at the upper limit of the span that can be reached by a single PI4P molecule; PI4P is estimated to be ~8 Å in its longest dimension, and it together with two salt bridges can potentially span 14 Å. Moreover, these residues project in different directions from the GAT helix bundle (Figure 2A). Therefore, the most straightforward interpretation is that these two residues bind different PI4P and that binding to multiple PI4P increases the binding avidity. On the other hand, if they were to bind the same PI4P, at least one residue will have to move into sterically favorable interaction distance. Allosteric regulation of GGA by phosphorylation has been reported previously (Ghosh and Kornfeld, 2003; McKay and Kahn, 2004), and a PI4P-induced conformational change is not precluded by the current structures of the GAT in the absence of PI4P.

Irrespective of how GGA binds PI4P, it is remarkable that despite GGA's engagement in the extensive network of parallel interactions at the TGN, a single point mutation in GGA's PI4P headgroup interactive site is sufficient to almost completely abrogate correct intracellular targeting. PI4P binding is therefore a critical upstream component of the GGA recruitment cascade.

GGA binds Ub, which is found on an increasing number of cargo proteins that traffic in the anterograde and retrograde directions (Dell'Angelica *et al.*, 2000; Hirst *et al.*, 2000; Doray *et al.*, 2002; Wahle *et al.*, 2005). PI4P promotes the recognition of the Ub-sorting signal by mammalian and yeast GGAs (Figure 5). Binding of one ligand (PI4P) may confer entropic advantage to the binding of another ligand (Ub). This scenario is different from that proposed for Ub and Rabaptin 5, which compete for GAT binding (Mattera *et al.*, 2004; Scott *et al.*, 2004; Shiba *et al.*, 2004). It has been shown previously by ITC that the heat generated by GGA3 GAT binding to Ub is contributed primarily by only one of the two known Ub-binding sites. This site, called site 1, is located upstream of the PI4P-binding residues identified here (Prag *et al.*, 2005; Figure 2, A and B). Because site 1 dominates in this assay (Prag *et al.*, 2005), our results suggest that PI4P promotes site 1 binding to Ub. Although not examined here, we speculate that site 2 might be modulated by PI4P as well, because the GGA1 PI4P-binding residue R265 is sandwiched between two critical site 2 Ub-binding residues (F264 and A267) that were identified by mutagenesis (Bilodeau *et al.*, 2004; Mattera *et al.*, 2004; Puertollano and Bonifacino, 2004; Akutsu *et al.*, 2005; Kawasaki *et al.*, 2005; Figure 2, A and B).

There has been much interest in the isoform-specific functions of the GGAs. Because GGA1 and GGA3 bind Ub with relatively low affinity, the approximately threefold increase in affinity by PI4P should facilitate their loading of the Ub cargoes at the TGN, which is enriched for PI4P. GGA2, which normally binds Ub even more weakly than GGA1 and GGA3 (Shiba *et al.*, 2004; Puertollano and Bonifacino, 2004), is also activated by PI4P to bind Ub (Figure 5A). Therefore, GGA2 can potentially sort ubiquitinated cargoes when it is placed in a PI4P-rich environment of the TGN. The different inherent affinities/avidities of the various GGAs for Ub, and their common activation by PI4P may allow fine-tuned regulation of ubiquitinated versus nonubiquitinated cargo sorting at the TGN.

The mechanism for increasing the affinity of the GAT domain for Ub remains to be determined. The data presented here shows for the first time that there is a direct relation between phosphoinositides and the recognition of a Ub-sorting signal during membrane trafficking. Thus, the trafficking of ubiquitinated cargoes may be directly regulated by the same phosphoinositide that recruits their cognate adaptors to the appropriate organelle membranes. This, together with reports that phosphoinositides tether a ubiquitin ligase to internal organelle membranes (Dunn *et al.*, 2004), and that GGA ubiquitination inhibits GGA binding to Ub cargoes (Hoeller *et al.*, 2006; Yogosawa *et al.*, 2006) underscore the emerging multifaceted roles of phosphoinositides in regulating membrane trafficking (Wenk and De Camilli, 2004).

ACKNOWLEDGMENTS

We thank J. Hurley (National Institutes of Health [NIH]), M. S. Robinson (University of Cambridge), and E. Lafer (UT San Antonio Health Science Center) for insightful discussions and many investigators, who were individually acknowledged in the text, for their generous gift of reagents. We acknowledge S. Sprang and C. Thomas (Department of Biochemistry and Protein Chemistry Core Facility, UT Southwestern) for assistance with the ITC experiments and Y. Mao for helpful discussions. This work is supported by NIH Grant GM055562, by the Robert A. Welch Foundation to H.L.Y., and by NIH Grant GM36548 to T.K.

REFERENCES

Akutsu, M., Kawasaki, M., Katoh, Y., Shiba, T., Yamaguchi, Y., Kato, R., Kato, K., Nakayama, K., and Wakatsuki, S. (2005). Structural basis for recognition of ubiquitinated cargo by Tom1-GAT domain. FEBS Lett. *579*, 5385–5391.

Barylko, B., Gerber, S. H., Binns, D. D., Grichine, N., Khvotchev, M., Sudhof, T. C., and Albanesi, J. P. (2001). A novel family of phosphatidylinositol 4-kinases conserved from yeast to humans. J. Biol. Chem. *276*, 7705–7708.

Behnia, R., and Munro, S. (2005). Organelle identity and the signposts for membrane traffic. Nature *438*, 597–604.

Bilodeau, P. S., Winistorfer, S. C., Allaman, M. M., Surendhran, K., Kearney, W. R., Robertson, A. D., and Piper, R. C. (2004). The GAT domains of clathrin-associated GGA proteins have two ubiquitin binding motifs. J. Biol. Chem. *279*, 54808–54816.

Bonifacino, J. S. (2004). The GGA proteins: adaptors on the move. Nat. Rev. Mol. Cell Biol. *5*, 23–32.

Carlton, J. G., and Cullen, P. J. (2005). Coincidence detection in phosphoinositide signaling. Trends Cell Biol. *15*, 540–547.

Collins, B. M., Watson, P. J., and Owen, D. J. (2003). The structure of the GGA1-GAT domain reveals the molecular basis for ARF binding and membrane association of GGAs. Dev. Cell *4*, 321–332.

Dell'Angelica, E. C., Puertollano, R., Mullins, C., Aguilar, R. C., Vargas, J. D., Hartnell, L. M., and Bonifacino, J. S. (2000). GGAs: a family of ADP ribosylation factor-binding proteins related to adaptors and associated with the Golgi complex. J. Cell Biol. *149*, 81–94.

Doray, B., Ghosh, P., Griffith, J., Geuze, H. J., and Kornfeld, S. (2002). Cooperation of GGAs and AP-1 in packaging MPRs at the trans-Golgi network. Science *297*, 1700–1703.

Dunn, R., Klos, D. A., Adler, A. S., and Hicke, L. (2004). The C2 domain of the Rsp5 ubiquitin ligase binds membrane phosphoinositides and directs ubiquitination of endosomal cargo. J. Cell Biol. *165*, 135–144.

Duronio, R. J., Jackson-Machelski, E., Heuckeroth, R. O., Olins, P. O., Devine, C. S., Yonemoto, W., Slice, L. W., Taylor, S. S., and Gordon, J. I. (1990). Protein N-myristoylation in *Escherichia coli*: reconstitution of a eukaryotic protein modification in bacteria. Proc. Natl. Acad. Sci. USA *87*, 1506–1510.

Franco, M., Chardin, P., Chabre, M., and Paris, S. (1995). Myristoylation of ADP-ribosylation factor 1 facilitates nucleotide exchange at physiological Mg levels. J. Biol. Chem. *270*, 1337–1341.

Ghosh, P., Griffith, J., Geuze, H. J., and Kornfeld, S. (2003). Mammalian GGAs act together to sort mannose 6-phosphate receptors. J. Cell Biol. *163*, 755–766.

Godi, A., Di Campli, A., Konstantakopoulos, A., Di Tullio, G., Alessi, D. R., Kular, G. S., Daniele, T., Marra, P., Lucocq, J. M., and De Matteis, M. A. (2004). FAPPs control Golgi-to-cell-surface membrane traffic by binding to ARF and PtdIns(4)P. Nat. Cell Biol. *6*, 393–404.

Heldwein, E. E., Macia, E., Wang, J., Yin, H. L., Kirchhausen, T., and Harrison, S. C. (2004). Crystal structure of the clathrin adaptor protein 1 core. Proc. Natl. Acad. Sci. USA *101*, 14108–14113.

Hirsch, D. S., Stanley, K. T., Chen, L.-X., Jacques, K. M., Puertollano, R., and Randazzo, P. A. (2003). Arf regulates interaction of GGA with mannose-6-phosphate receptor. Traffic *4*, 26–35.

Hirst, J., Lui, W. W., Bright, N. A., Totty, N., Seaman, M. N., and Robinson, M. S. (2000). A family of proteins with gamma-adaptin and VHS domains that facilitate trafficking between the trans-Golgi network and the vacuole/lysosome. J. Cell Biol. *149*, 67–80.

Hirst, J., Motley, A., Harasaki, K., Peak Chew, S. Y., and Robinson, M. S. (2003). EpsinR: an ENTH domain-containing protein that interacts with AP-1. Mol. Biol. Cell *14*, 625–641.

Hoeller, D. *et al.* (2006). Regulation of ubiquitin-binding proteins by monoubiquitination. Nat. Cell Biol. *8*, 163–169.

Kawasaki, M. *et al.* (2005). Molecular mechanism of ubiquitin recognition by GGA3 GAT domain. Genes Cells *10*, 639–654.

Kim, Y., Deng, Y., and Philpott, C.C. (2007). GGA2- and ubiquitin-dependent trafficking of Arn1, the ferrichrome transporter of *Saccharomyces cerevisiae.* Mol. Biol. Cell *18*, 1790–1802.

Levine, T. P., and Munro, S. (2002). Targeting of Golgi-specific pleckstrin homology domains involves both PtdIns 4-kinase-dependent and -independent components. Curr. Biol. *12*, 695–704.

Mao, Y., Chen, J., Maynard, J. A., Zhang, B., and Quiocho, F. A. (2001). A novel all helix fold of the AP180 amino-terminal domain for phosphoinositide binding and clathrin assembly in synaptic vesicle endocytosis. Cell *104*, 433–440.

Mattera, R., Puertollano, R., Smith, W. J., and Bonifacino, J. S. (2004). The trihelical bundle subdomain of the GGA proteins interacts with multiple partners through overlapping but distinct sites. J. Biol. Chem. *279*, 31409–31418.

McKay, M. M., and Kahn, R. A. (2004). Multiple phosphorylation events regulate the subcellular localization of GGA1. Traffic *5*, 102–116.

Prag, G., Lee, S., Mattera, R., Arighi, C. N., Beach, B. M., Bonifacino, J. S., and Hurley, J. H. (2005). Structural mechanism for ubiquitinated-cargo recognition by the Golgi-localized, gamma-ear-containing, ADP-ribosylation-factor-binding proteins. Proc. Natl. Acad. Sci. USA *102*, 2334–2339.

Puertollano, R., and Bonifacino, J. S. (2004). Interactions of GGA3 with the ubiquitin sorting machinery. Nat. Cell Biol. *6*, 244–251.

Puertollano, R., Randazzo, P. A., Presley, J. F., Hartnell, L. M., and Bonifacino, J. S. (2001). The GGAs promote ARF-dependent recruitment of clathrin to the TGN. Cell *105*, 93–102.

Scott, P. M., Bilodeau, P. S., Zhdankina, O., Winistorfer, S. C., Hauglund, M. J., Allaman, M. M., Kearney, W. R., Robertson, A. D., Boman, A. L., and Piper, R. C. (2004). GGA proteins bind ubiquitin to facilitate sorting at the trans-Golgi network. Nat. Cell Biol. *6*, 252–259.

Shiba, T., Kawasaki, M., Takatsu, H., Nogi, T., Matsugaki, N., Igarashi, N., Suzuki, M., Kato, R., Nakayama, K., and Wakatsuki, S. (2003). Molecular mechanism of membrane recruitment of GGA by ARF in lysosomal protein transport. Nat. Struct. Biol. *10*, 386–393.

Shiba, Y., Katoh, Y., Shiba, T., Yoshino, K., Takatsu, H., Kobayashi, H., Shin, H. W., Wakatsuki, S., and Nakayama, K. (2004). GAT (GGA and Tom1) domain responsible for ubiquitin binding and ubiquitination. J. Biol. Chem. *279*, 7105–7111.

Suer, S., Misra, S., Saidi, L. F., and Hurley, J. H. (2003). Structure of the GAT domain of human GGA 1, a syntaxin amino-terminal domain fold in an endosomal trafficking adaptor. Proc. Natl. Acad. Sci. USA *100*, 4451–4456.

Takatsu, H., Yoshino, K., Toda, K., and Nakayama, K. (2002). GGA proteins associate with Golgi membranes through interaction between their GGAH domains and ADP-ribosylation factors. Biochem. J. *365*, 369–378.

Wahle, T., Prager, K., Raffler, N., Haass, C., Famulok, M., and Walter, J. (2005). GGA proteins regulate retrograde transport of BACE1 from endosomes to the trans-Golgi network. Mol. Cell Neurosci. *29*, 453–461.

Wang, Y. J., Wang, J., Sun, H. Q., Martinez, M., Sun, Y. X., Macia, E., Kirchhausen, T., Albanesi, J. P., Roth, M. G., and Yin, H. L. (2003). Phosphatidylinositol 4 phosphate regulates targeting of clathrin adaptor AP-1 complexes to the Golgi. Cell *114*, 299–310.

Wei, Y. J., Sun, H. Q., Yamamoto, M., Wlodarski, P., Kunii, K., Martinez, M., Barylko, B., Albanesi, J. P., and Yin, H. L. (2002). Type II phosphatidylinositol 4-kinase beta is a cytosolic and peripheral membrane protein that is recruited to the plasma membrane and activated by Rac-GTP. J. Biol. Chem. *277*, 46586–46593.

Wenk, M. R., and De Camilli, P. (2004). Protein-lipid interactions and phosphoinositide metabolism in membrane traffic: insights from vesicle recycling in nerve terminals. Proc. Natl. Acad. Sci. USA *101*, 8262–8269.

Yin, H. L., and Janmey, P. A. (2003). Phosphoinositide regulation of the actin cytoskeleton. Annu. Rev. Physiol. *65*, 761–789.

Yogosawa, S., Kawasaki, M., Wakatsuki, S., Kominami, E., Shiba, Y., Nakayama, K., Kohsaka, S., and Akazawa, C. (2006). Monoubiquitylation of GGA3 by hVPS18 regulates its ubiquitin-binding ability. Biochem. Biophys. Res. Commun. *350*, 82–90.

Yu, J. W., Mendrola, J. M., Audhya, A., Singh, S., Keleti, D., DeWald, D. B., Murray, D., Emr, S. D., and Lemmon, M. A. (2004). Genome-wide analysis of membrane targeting by *S. cerevisiae* pleckstrin homology domains. Mol. Cell *13*, 677–688.